Evidence for direct *CP* violation from Dalitz-plot analysis of $B^{\pm} \to K^{\pm}\pi^{\mp}\pi^{\pm}$

B. Aubert,[1] M. Bona,[1] Y. Karyotakis,[1] J. P. Lees,[1] V. Poireau,[1] E. Prencipe,[1] X. Prudent,[1] V. Tisserand,[1] J. Garra Tico,[2] E. Grauges,[2] L. Lopez,[3] A. Palano,[3] M. Pappagallo,[3] G. Eigen,[4] B. Stugu,[4] L. Sun,[4] G. S. Abrams,[5] M. Battaglia,[5] D. N. Brown,[5] J. Button-Shafer,[5] R. N. Cahn,[5] R. G. Jacobsen,[5] J. A. Kadyk,[5] L. T. Kerth,[5] Yu. G. Kolomensky,[5] G. Kukartsev,[5] G. Lynch,[5] I. L. Osipenkov,[5] M. T. Ronan,[5] K. Tackmann,[5] T. Tanabe,[5] W. A. Wenzel,[5] C. M. Hawkes,[6] N. Soni,[6] A. T. Watson,[6] H. Koch,[7] T. Schroeder,[7] D. Walker,[8] D. J. Asgeirsson,[9] T. Cuhadar-Donszelmann,[9] B. G. Fulsom,[9] C. Hearty,[9] T. S. Mattison,[9] J. A. McKenna,[9] M. Barrett,[10] A. Khan,[10] M. Saleem,[10] L. Teodorescu,[10] V. E. Blinov,[11] A. D. Bukin,[11] A. R. Buzykaev,[11] V. P. Druzhinin,[11] V. B. Golubev,[11] A. P. Onuchin,[11] S. I. Serednyakov,[11] Yu. I. Skovpen,[11] E. P. Solodov,[11] K. Yu. Todyshev,[11] M. Bondioli,[12] S. Curry,[12] I. Eschrich,[12] D. Kirkby,[12] A. J. Lankford,[12] P. Lund,[12] M. Mandelkern,[12] E. C. Martin,[12] D. P. Stoker,[12] S. Abachi,[13] C. Buchanan,[13] J. W. Gary,[14] F. Liu,[14] O. Long,[14] B. C. Shen,[14,*] G. M. Vitug,[14] Z. Yasin,[14] L. Zhang,[14] V. Sharma,[15] C. Campagnari,[16] T. M. Hong,[16] D. Kovalskyi,[16] M. A. Mazur,[16] J. D. Richman,[16] T. W. Beck,[17] A. M. Eisner,[17] C. J. Flacco,[17] C. A. Heusch,[17] J. Kroseberg,[17] W. S. Lockman,[17] T. Schalk,[17] B. A. Schumm,[17] A. Seiden,[17] L. Wang,[17] M. G. Wilson,[17] L. O. Winstrom,[17] C. H. Cheng,[18] D. A. Doll,[18] B. Echenard,[18] F. Fang,[18] D. G. Hitlin,[18] I. Narsky,[18] T. Piatenko,[18] F. C. Porter,[18] R. Andreassen,[19] G. Mancinelli,[19] B. T. Meadows,[19] K. Mishra,[19] M. D. Sokoloff,[19] F. Blanc,[20] P. C. Bloom,[20] W. T. Ford,[20] A. Gaz,[20] J. F. Hirschauer,[20] A. Kreisel,[20] M. Nagel,[20] U. Nauenberg,[20] A. Olivas,[20] J. G. Smith,[20] K. A. Ulmer,[20] S. R. Wagner,[20] R. Ayad,[21,+] A. M. Gabareen,[21] A. Soffer,[21,‡] W. H. Toki,[21] R. J. Wilson,[21] D. D. Altenburg,[22] E. Feltresi,[22] A. Hauke,[22] H. Jasper,[22] M. Karbach,[22] J. Merkel,[22] A. Petzold,[22] B. Spaan,[22] K. Wacker,[22] V. Klose,[23] M. J. Kobel,[23] H. M. Lacker,[23] W. F. Mader,[23] R. Nogowski,[23] K. R. Schubert,[23] R. Schwierz,[23] J. E. Sundermann,[23] A. Volk,[23] D. Bernard,[24] G. R. Bonneaud,[24] E. Latour,[24] Ch. Thiebaux,[24] M. Verderi,[24] P. J. Clark,[25] W. Gradl,[25] S. Playfer,[25] J. E. Watson,[25] M. Andreotti,[26] D. Bettoni,[26] C. Bozzi,[26] R. Calabrese,[26] A. Cecchi,[26] G. Cibinetto,[26] P. Franchini,[26] E. Luppi,[26] M. Negrini,[26] A. Petrella,[26] L. Piemontese,[26] V. Santoro,[26] F. Anulli,[27] R. Baldini-Ferroli,[27] A. Calcaterra,[27] R. de Sangro,[27] G. Finocchiaro,[27] S. Pacetti,[27] P. Patteri,[27] I. M. Peruzzi,[27,§] M. Piccolo,[27] M. Rama,[27] A. Zallo,[27] A. Buzzo,[28] R. Contri,[28] M. Lo Vetere,[28] M. M. Macri,[28] M. R. Monge,[28] S. Passaggio,[28] C. Patrignani,[28] E. Robutti,[28] A. Santroni,[28] S. Tosi,[28] K. S. Chaisanguanthum,[29] M. Morii,[29] R. S. Dubitzky,[30] J. Marks,[30] S. Schenk,[30] U. Uwer,[30] D. J. Bard,[31] P. D. Dauncey,[31] J. A. Nash,[31] W. Panduro Vazquez,[31] M. Tibbetts,[31] P. K. Behera,[32] X. Chai,[32] M. J. Charles,[32] U. Mallik,[32] J. Cochran,[33] H. B. Crawley,[33] L. Dong,[33] W. T. Meyer,[33] S. Prell,[33] E. I. Rosenberg,[33] A. E. Rubin,[33] Y. Y. Gao,[34] A. V. Gritsan,[34] Z. J. Guo,[34] C. K. Lae,[34] A. G. Denig,[35] M. Fritsch,[35] G. Schott,[35] N. Arnaud,[36] J. Béquilleux,[36] A. D'Orazio,[36] M. Davier,[36] J. Firmino da Costa,[36] G. Grosdidier,[36] A. Höcker,[36] V. Lepeltier,[36] F. Le Diberder,[36] A. M. Lutz,[36] S. Pruvot,[36] P. Roudeau,[36] M. H. Schune,[36] J. Serrano,[36] V. Sordini,[36] A. Stocchi,[36] W. F. Wang,[36] G. Wormser,[36] D. J. Lange,[37] D. M. Wright,[37] I. Bingham,[38] J. P. Burke,[38] C. A. Chavez,[38] J. R. Fry,[38] E. Gabathuler,[38] R. Gamet,[38] D. E. Hutchcroft,[38] D. J. Payne,[38] C. Touramanis,[38] A. J. Bevan,[39] K. A. George,[39] F. Di Lodovico,[39] R. Sacco,[39] M. Sigamani,[39] G. Cowan,[40] H. U. Flaecher,[40] D. A. Hopkins,[40] S. Paramesvaran,[40] F. Salvatore,[40] A. C. Wren,[40] D. N. Brown,[41] C. L. Davis,[41] K. E. Alwyn,[42] N. R. Barlow,[42] R. J. Barlow,[42] Y. M. Chia,[42] C. L. Edgar,[42] G. D. Lafferty,[42] T. J. West,[42] J. I. Yi,[42] J. Anderson,[43] C. Chen,[43] A. Jawahery,[43] D. A. Roberts,[43] G. Simi,[43] J. M. Tuggle,[43] C. Dallapiccola,[44] S. S. Hertzbach,[44] X. Li,[44] E. Salvati,[44] S. Saremi,[44] R. Cowan,[45] D. Dujmic,[45] P. H. Fisher,[45] K. Koeneke,[45] G. Sciolla,[45] M. Spitznagel,[45] F. Taylor,[45] R. K. Yamamoto,[45] M. Zhao,[45] S. E. Mclachlin,[46,*] P. M. Patel,[46] S. H. Robertson,[46] A. Lazzaro,[47] V. Lombardo,[47] F. Palombo,[47] J. M. Bauer,[48] L. Cremaldi,[48] V. Eschenburg,[48] R. Godang,[48] R. Kroeger,[48] D. A. Sanders,[48] D. J. Summers,[48] H. W. Zhao,[48] S. Brunet,[49] D. Côté,[49] M. Simard,[49] P. Taras,[49] F. B. Viaud,[49] H. Nicholson,[50] G. De Nardo,[51] L. Lista,[51] D. Monorchio,[51] C. Sciacca,[51] M. A. Baak,[52] G. Raven,[52] H. L. Snoek,[52] C. P. Jessop,[53] K. J. Knoepfel,[53] J. M. LoSecco,[53] G. Benelli,[54] L. A. Corwin,[54] K. Honscheid,[54] H. Kagan,[54] R. Kass,[54] J. P. Morris,[54] A. M. Rahimi,[54] J. J. Regensburger,[54] S. J. Sekula,[54] Q. K. Wong,[54] N. L. Blount,[55] J. Brau,[55] R. Frey,[55] O. Igonkina,[55] J. A. Kolb,[55] M. Lu,[55] R. Rahmat,[55] N. B. Sinev,[55] D. Strom,[55] J. Strube,[55] E. Torrence,[55] G. Castelli,[56] N. Gagliardi,[56] M. Margoni,[56] M. Morandin,[56] M. Posocco,[56] M. Rotondo,[56] F. Simonetto,[56] R. Stroili,[56] C. Voci,[56] P. del Amo Sanchez,[57] E. Ben-Haim,[57] H. Briand,[57] G. Calderini,[57] J. Chauveau,[57] P. David,[57] L. Del Buono,[57] O. Hamon,[57] Ph. Leruste,[57] J. Ocariz,[57] A. Perez,[57] J. Prendki,[57] L. Gladney,[58] M. Biasini,[59] R. Covarelli,[59] E. Manoni,[59] C. Angelini,[60] G. Batignani,[60] S. Bettarini,[60] M. Carpinelli,[60,‖] A. Cervelli,[60] F. Forti,[60] M. A. Giorgi,[60] A. Lusiani,[60] G. Marchiori,[60] M. Morganti,[60] N. Neri,[60] E. Paoloni,[60] G. Rizzo,[60] J. J. Walsh,[60] J. Biesiada,[61] D. Lopes Pegna,[61] C. Lu,[61] J. Olsen,[61] A. J. S. Smith,[61] A. V. Telnov,[61] E. Baracchini,[62] G. Cavoto,[62] D. del Re,[62] E. Di Marco,[62] R. Faccini,[62] F. Ferrarotto,[62]

F. Ferroni,[62] M. Gaspero,[62] P. D. Jackson,[62] L. Li Gioi,[62] M. A. Mazzoni,[62] S. Morganti,[62] G. Piredda,[62] F. Polci,[62] F. Renga,[62] C. Voena,[62] M. Ebert,[63] T. Hartmann,[63] H. Schröder,[63] R. Waldi,[63] T. Adye,[64] B. Franek,[64] E. O. Olaiya,[64] W. Roethel,[64] F. F. Wilson,[64] S. Emery,[65] M. Escalier,[65] L. Esteve,[65] A. Gaidot,[65] S. F. Ganzhur,[65] G. Hamel de Monchenault,[65] W. Kozanecki,[65] G. Vasseur,[65] Ch. Yèche,[65] M. Zito,[65] X. R. Chen,[66] H. Liu,[66] W. Park,[66] M. V. Purohit,[66] R. M. White,[66] J. R. Wilson,[66] M. T. Allen,[67] D. Aston,[67] R. Bartoldus,[67] P. Bechtle,[67] J. F. Benitez,[67] R. Cenci,[67] J. P. Coleman,[67] M. R. Convery,[67] J. C. Dingfelder,[67] J. Dorfan,[67] G. P. Dubois-Felsmann,[67] W. Dunwoodie,[67] R. C. Field,[67] S. J. Gowdy,[67] M. T. Graham,[67] P. Grenier,[67] C. Hast,[67] W. R. Innes,[67] J. Kaminski,[67] M. H. Kelsey,[67] H. Kim,[67] P. Kim,[67] M. L. Kocian,[67] D. W. G. S. Leith,[67] S. Li,[67] B. Lindquist,[67] S. Luitz,[67] V. Luth,[67] H. L. Lynch,[67] D. B. MacFarlane,[67] H. Marsiske,[67] R. Messner,[67] D. R. Muller,[67] H. Neal,[67] S. Nelson,[67] C. P. O'Grady,[67] I. Ofte,[67] A. Perazzo,[67] M. Perl,[67] B. N. Ratcliff,[67] A. Roodman,[67] A. A. Salnikov,[67] R. H. Schindler,[67] J. Schwiening,[67] A. Snyder,[67] D. Su,[67] M. K. Sullivan,[67] K. Suzuki,[67] S. K. Swain,[67] J. M. Thompson,[67] J. Va'vra,[67] A. P. Wagner,[67] M. Weaver,[67] C. A. West,[67] W. J. Wisniewski,[67] M. Wittgen,[67] D. H. Wright,[67] H. W. Wulsin,[67] A. K. Yarritu,[67] K. Yi,[67] C. C. Young,[67] V. Ziegler,[67] P. R. Burchat,[68] A. J. Edwards,[68] S. A. Majewski,[68] T. S. Miyashita,[68] B. A. Petersen,[68] L. Wilden,[68] S. Ahmed,[69] M. S. Alam,[69] R. Bula,[69] J. A. Ernst,[69] B. Pan,[69] M. A. Saeed,[69] S. B. Zain,[69] S. M. Spanier,[70] B. J. Wogsland,[70] R. Eckmann,[71] J. L. Ritchie,[71] A. M. Ruland,[71] C. J. Schilling,[71] R. F. Schwitters,[71] B. W. Drummond,[72] J. M. Izen,[72] X. C. Lou,[72] S. Ye,[72] F. Bianchi,[73] D. Gamba,[73] M. Pelliccioni,[73] M. Bomben,[74] L. Bosisio,[74] C. Cartaro,[74] G. Della Ricca,[74] L. Lanceri,[74] L. Vitale,[74] V. Azzolini,[75] N. Lopez-March,[75] F. Martinez-Vidal,[75] D. A. Milanes,[75] A. Oyanguren,[75] J. Albert,[76] Sw. Banerjee,[76] B. Bhuyan,[76] H. H. F. Choi,[76] K. Hamano,[76] R. Kowalewski,[76] M. J. Lewczuk,[76] I. M. Nugent,[76] J. M. Roney,[76] R. J. Sobie,[76] T. J. Gershon,[77] P. F. Harrison,[77] J. Ilic,[77] T. E. Latham,[77] G. B. Mohanty,[77] H. R. Band,[78] X. Chen,[78] S. Dasu,[78] K. T. Flood,[78] Y. Pan,[78] M. Pierini,[78] R. Prepost,[78] C. O. Vuosalo,[78] and S. L. Wu[78]

(The *BABAR* Collaboration)

[1]*Laboratoire de Physique des Particules, IN2P3/CNRS et Université de Savoie, F-74941 Annecy-Le-Vieux, France*
[2]*Universitat de Barcelona, Facultat de Fisica, Departament ECM, E-08028 Barcelona, Spain*
[3]*Università di Bari, Dipartimento di Fisica and INFN, I-70126 Bari, Italy*
[4]*University of Bergen, Institute of Physics, N-5007 Bergen, Norway*
[5]*Lawrence Berkeley National Laboratory and University of California, Berkeley, California 94720, USA*
[6]*University of Birmingham, Birmingham, B15 2TT, United Kingdom*
[7]*Ruhr Universität Bochum, Institut für Experimentalphysik 1, D-44780 Bochum, Germany*
[8]*University of Bristol, Bristol BS8 1TL, United Kingdom*
[9]*University of British Columbia, Vancouver, British Columbia, Canada V6T 1Z1*
[10]*Brunel University, Uxbridge, Middlesex UB8 3PH, United Kingdom*
[11]*Budker Institute of Nuclear Physics, Novosibirsk 630090, Russia*
[12]*University of California at Irvine, Irvine, California 92697, USA*
[13]*University of California at Los Angeles, Los Angeles, California 90024, USA*
[14]*University of California at Riverside, Riverside, California 92521, USA*
[15]*University of California at San Diego, La Jolla, California 92093, USA*
[16]*University of California at Santa Barbara, Santa Barbara, California 93106, USA*
[17]*University of California at Santa Cruz, Institute for Particle Physics, Santa Cruz, California 95064, USA*
[18]*California Institute of Technology, Pasadena, California 91125, USA*
[19]*University of Cincinnati, Cincinnati, Ohio 45221, USA*
[20]*University of Colorado, Boulder, Colorado 80309, USA*
[21]*Colorado State University, Fort Collins, Colorado 80523, USA*
[22]*Technische Universität Dortmund, Fakultät Physik, D-44221 Dortmund, Germany*
[23]*Technische Universität Dresden, Institut für Kern- und Teilchenphysik, D-01062 Dresden, Germany*
[24]*Laboratoire Leprince-Ringuet, CNRS/IN2P3, Ecole Polytechnique, F-91128 Palaiseau, France*
[25]*University of Edinburgh, Edinburgh EH9 3JZ, United Kingdom*
[26]*Università di Ferrara, Dipartimento di Fisica and INFN, I-44100 Ferrara, Italy*
[27]*Laboratori Nazionali di Frascati dell'INFN, I-00044 Frascati, Italy*
[28]*Università di Genova, Dipartimento di Fisica and INFN, I-16146 Genova, Italy*
[29]*Harvard University, Cambridge, Massachusetts 02138, USA*
[30]*Universität Heidelberg, Physikalisches Institut, Philosophenweg 12, D-69120 Heidelberg, Germany*
[31]*Imperial College London, London, SW7 2AZ, United Kingdom*
[32]*University of Iowa, Iowa City, Iowa 52242, USA*

[33]*Iowa State University, Ames, Iowa 50011-3160, USA*
[34]*Johns Hopkins University, Baltimore, Maryland 21218, USA*
[35]*Universität Karlsruhe, Institut für Experimentelle Kernphysik, D-76021 Karlsruhe, Germany*
[36]*Laboratoire de l'Accélérateur Linéaire, IN2P3/CNRS et Université Paris-Sud 11, Centre Scientifique d'Orsay, B. P. 34, F-91898 ORSAY Cedex, France*
[37]*Lawrence Livermore National Laboratory, Livermore, California 94550, USA*
[38]*University of Liverpool, Liverpool L69 7ZE, United Kingdom*
[39]*Queen Mary, University of London, E1 4NS, United Kingdom*
[40]*University of London, Royal Holloway and Bedford New College, Egham, Surrey TW20 0EX, United Kingdom*
[41]*University of Louisville, Louisville, Kentucky 40292, USA*
[42]*University of Manchester, Manchester M13 9PL, United Kingdom*
[43]*University of Maryland, College Park, Maryland 20742, USA*
[44]*University of Massachusetts, Amherst, Massachusetts 01003, USA*
[45]*Massachusetts Institute of Technology, Laboratory for Nuclear Science, Cambridge, Massachusetts 02139, USA*
[46]*McGill University, Montréal, Québec, Canada H3A 2T8*
[47]*Università di Milano, Dipartimento di Fisica and INFN, I-20133 Milano, Italy*
[48]*University of Mississippi, University, Mississippi 38677, USA*
[49]*Université de Montréal, Physique des Particules, Montréal, Québec, Canada H3C 3J7*
[50]*Mount Holyoke College, South Hadley, Massachusetts 01075, USA*
[51]*Università di Napoli Federico II, Dipartimento di Scienze Fisiche and INFN, I-80126, Napoli, Italy*
[52]*NIKHEF, National Institute for Nuclear Physics and High Energy Physics, NL-1009 DB Amsterdam, The Netherlands*
[53]*University of Notre Dame, Notre Dame, Indiana 46556, USA*
[54]*Ohio State University, Columbus, Ohio 43210, USA*
[55]*University of Oregon, Eugene, Oregon 97403, USA*
[56]*Università di Padova, Dipartimento di Fisica and INFN, I-35131 Padova, Italy*
[57]*Laboratoire de Physique Nucléaire et de Hautes Energies, IN2P3/CNRS, Université Pierre et Marie Curie-Paris6, Université Denis Diderot-Paris7, F-75252 Paris, France*
[58]*University of Pennsylvania, Philadelphia, Pennsylvania 19104, USA*
[59]*Università di Perugia, Dipartimento di Fisica and INFN, I-06100 Perugia, Italy*
[60]*Università di Pisa, Dipartimento di Fisica, Scuola Normale Superiore and INFN, I-56127 Pisa, Italy*
[61]*Princeton University, Princeton, New Jersey 08544, USA*
[62]*Università di Roma La Sapienza, Dipartimento di Fisica and INFN, I-00185 Roma, Italy*
[63]*Universität Rostock, D-18051 Rostock, Germany*
[64]*Rutherford Appleton Laboratory, Chilton, Didcot, Oxon, OX11 0QX, United Kingdom*
[65]*DSM/Dapnia, CEA/Saclay, F-91191 Gif-sur-Yvette, France*
[66]*University of South Carolina, Columbia, South Carolina 29208, USA*
[67]*Stanford Linear Accelerator Center, Stanford, California 94309, USA*
[68]*Stanford University, Stanford, California 94305-4060, USA*
[69]*State University of New York, Albany, New York 12222, USA*
[70]*University of Tennessee, Knoxville, Tennessee 37996, USA*
[71]*University of Texas at Austin, Austin, Texas 78712, USA*
[72]*University of Texas at Dallas, Richardson, Texas 75083, USA*
[73]*Università di Torino, Dipartimento di Fisica Sperimentale and INFN, I-10125 Torino, Italy*
[74]*Università di Trieste, Dipartimento di Fisica and INFN, I-34127 Trieste, Italy*
[75]*IFIC, Universitat de Valencia-CSIC, E-46071 Valencia, Spain*
[76]*University of Victoria, Victoria, British Columbia, Canada V8W 3P6*
[77]*Department of Physics, University of Warwick, Coventry CV4 7AL, United Kingdom*
[78]*University of Wisconsin, Madison, Wisconsin 53706, USA*
(Received 31 March 2008; published 14 July 2008)

We report a Dalitz-plot analysis of the charmless hadronic decays of charged B mesons to the final state $K^{\pm}\pi^{\mp}\pi^{\pm}$. Using a sample of $(383.2 \pm 4.2) \times 10^6$ $B\bar{B}$ pairs collected by the *BABAR* detector, we measure *CP*-averaged branching fractions and direct *CP* asymmetries for intermediate resonant and nonresonant

[*]Deceased.
[+]Now at Temple University, Philadelphia, PA 19122, USA.
[‡]Now at Tel Aviv University, Tel Aviv, 69978, Israel.
[§]Also with Università di Perugia, Dipartimento di Fisica, Perugia, Italy.
[‖]Also with Università di Sassari, Sassari, Italy.

contributions. We find evidence for direct CP violation in the decay $B^\pm \to \rho^0(770)K^\pm$, with a CP-violation parameter $A_{CP} = (+44 \pm 10 \pm 4^{+5}_{-13})\%$.

DOI: 10.1103/PhysRevD.78.012004 PACS numbers: 13.25.Hw, 11.30.Er, 12.15.Hh

I. INTRODUCTION

The Kobayashi-Maskawa mechanism of CP nonconservation [1] has, in recent years, been confirmed through observations of direct CP violation in the kaon system [2,3] and of both mixing-induced [4,5] and direct [6] CP violation in the B meson system. However, it is striking that despite an enormous experimental effort [7,8], no observation of CP violation in the decay of any charged particle has yet been made. In some cases, for example, in $B^\pm \to \pi^0 K^\pm$ [9,10], the absence of an asymmetry is difficult to understand theoretically [11–16]. The search for such effects is therefore a priority for studies of the weak interaction.

Several theoretical investigations have suggested that large CP asymmetries may be observed in $B^\pm \to \rho^0(770)K^\pm$ decays [17–25]. Because of the large width of the ρ^0 meson, this channel must be studied using a Dalitz-plot analysis of the $K^\pm\pi^\mp\pi^\pm$ final state. Previous measurements found $A_{CP}(B^\pm \to \rho^0(770)K^\pm) = (+32 \pm 13 \pm 6^{+8}_{-5})\%$ [26] and $A_{CP}(B^\pm \to \rho^0(770)K^\pm) = (+30 \pm 11 \pm 2^{+11}_{-4})\%$ [27] (where the errors are statistical, systematic, and model-dependent, respectively), indicating evidence for CP violation in this decay, and leaving a strong need for more precise and conclusive studies.

Several other considerations motivate a precise analysis of $B^\pm \to K^\pm\pi^\mp\pi^\pm$ decays. The CP asymmetries in the decays $B^+ \to K^{*0}(892)\pi^+$, $B^+ \to K_0^{*0}(1430)\pi^+$, and $B^+ \to K_2^{*0}(1430)\pi^+$ are predicted to be negligible [19,20] compared to the current precision, since these are mediated by $b \to s$ loop (penguin) transitions only, with no $b \to u$ tree component. A significant CP-violation effect in any of these channels would therefore provide a signature of new physics. On the other hand, decays such as $B^+ \to \rho^0 K^+$ may have comparable contributions from both tree and penguin amplitudes, and their interference is sensitive to their relative weak (CP violating) phase difference γ. Results from amplitude analyses of $B^\pm \to K^\pm\pi^\mp\pi^\pm$ and other $B \to K\pi\pi$ decays [28–30] can be combined to constrain the hadronic parameters and allow a relatively clean determination of γ [31–36].

Understanding the dynamics of the $B^\pm \to K^\pm\pi^\mp\pi^\pm$ Dalitz plot is also a priority. Previous studies have left unresolved the nature of a structure peaking at invariant mass around 1300 MeV/c^2 in the $\pi^+\pi^-$ spectrum (denoted $f_X(1300)$ in this work). Similar enhancements have also been seen at low K^+K^- invariant masses in $B \to KKK$ [37–39] and $B^\pm \to K^\pm K^\mp \pi^\pm$ [40] decays. The origin of these structures has aroused considerable interest among theorists [41–45], as it is of great importance in the understanding of low energy spectroscopy [46].

In this paper we present results from an amplitude analysis of $B^\pm \to K^\pm\pi^\mp\pi^\pm$ decays based on a 347.5 fb^{-1} data sample containing $(383.2 \pm 4.2) \times 10^6$ $B\bar{B}$ pairs ($N_{B\bar{B}}$). Compared to our previous publication [26], we have increased the data sample by 70%, included several improvements in reconstruction algorithms that enhance the signal efficiency, made several modifications to the analysis to increase the sensitivity to direct CP-violating effects (for example, by including more discriminating variables in the maximum likelihood fit), and improved our model of the Dalitz-plot structure. Moreover, we have developed a novel parametrization of the coefficients used in the fit that ensures good statistical behavior of the fitted parameters.

The data were collected with the *BABAR* detector [47] at the SLAC PEP-II asymmetric-energy e^+e^- storage rings [48] operating at the $\Upsilon(4S)$ resonance with center-of-mass (CM) energy of $\sqrt{s} = 10.58$ GeV. An additional total integrated luminosity of 36.6 fb^{-1} was recorded 40 MeV below the $\Upsilon 4S$ resonance ("off-peak" data) and was used to study backgrounds from continuum production.

II. AMPLITUDE ANALYSIS FORMALISM

A number of intermediate states contribute to the decay $B^\pm \to K^\pm\pi^\mp\pi^\pm$. Their individual contributions are obtained from a maximum likelihood fit of the distribution of events in the Dalitz plot formed from the two variables $m^2_{K\pi} \equiv m^2_{K^\pm\pi^\mp}$ and $m^2_{\pi\pi} \equiv m^2_{\pi^\pm\pi^\mp}$. The total signal amplitudes for B^+ and B^- decays are given, in the isobar formalism (see for example [49–51]), by:

$$A = A(m^2_{K\pi}, m^2_{\pi\pi}) = \sum_j c_j F_j(m^2_{K\pi}, m^2_{\pi\pi}), \qquad (1)$$

$$\bar{A} = \bar{A}(m^2_{K\pi}, m^2_{\pi\pi}) = \sum_j \bar{c}_j \bar{F}_j(m^2_{K\pi}, m^2_{\pi\pi}),. \qquad (2)$$

The complex coefficient for a given decay mode j is c_j and is measured relative to one of the contributing channels ($K^{*0}(892)$ in this analysis). The c_j contain all the weak phase dependence and so $F_j \equiv \bar{F}_j$. The distributions F_j describe the dynamics of the decay amplitudes and are the product of an invariant mass term (R_j), two Blatt-Weisskopf barrier form factors ($X_J(z)$) [52], and an angular function (T_j):

$$F_j = R_j \times X_J(p^\star) \times X_J(q) \times T_j, \qquad (3)$$

where J is the spin of the resonance, q is the momentum of either daughter in the rest frame of the resonance, and $p^\star$ is the momentum of the bachelor particle in the rest frame of

the B. The F_j are normalized over the entire Dalitz plot:

$$\iint |F_j(m^2_{K\pi}, m^2_{\pi\pi})|^2 dm^2_{K\pi} dm^2_{\pi\pi} = 1. \quad (4)$$

The Blatt-Weisskopf barrier form factors are given by:

$$X_{J=0}(z) = 1, \quad (5)$$

$$X_{J=1}(z) = \sqrt{1/(1 + (zr_{\rm BW})^2)}, \quad (6)$$

$$X_{J=2}(z) = \sqrt{1/((zr_{\rm BW})^4 + 3(zr_{\rm BW})^2 + 9)}, \quad (7)$$

where $r_{\rm BW}$, the meson radius parameter, is taken to be (4.0 ± 1.0) $(\mathrm{GeV}/c)^{-1}$ [53].

For most resonances in this analysis the R_j are taken to be relativistic Breit-Wigner line shapes:

$$R_j(m) = \frac{1}{(m_0^2 - m^2) - im_0\Gamma(m)}, \quad (8)$$

where m_0 is the nominal mass of the resonance and $\Gamma(m)$ is the mass-dependent width. In the general case of a spin-J resonance, the latter can be expressed as

$$\Gamma(m) = \Gamma_0 \left(\frac{q}{q_0}\right)^{2J+1} \left(\frac{m_0}{m}\right) \frac{X_J^2(q)}{X_J^2(q_0)}. \quad (9)$$

The symbol Γ_0 denotes the nominal width of the resonance. The values of m_0 and Γ_0 are obtained from standard tables [7]. The symbol q_0 denotes the value of q when $m = m_0$.

For the $f_0(980)$ line shape the Flatté form [54] is used. In this case the mass-dependent width is given by the sum of the widths in the $\pi\pi$ and KK systems:

$$\Gamma(m) = \Gamma_{\pi\pi}(m) + \Gamma_{KK}(m), \quad (10)$$

where

$$\Gamma_{\pi\pi}(m) = g_\pi \left(\frac{1}{3}\sqrt{1 - 4m^2_{\pi^0}/m^2} + \frac{2}{3}\sqrt{1 - 4m^2_{\pi^\pm}/m^2}\right), \quad (11)$$

$$\Gamma_{KK}(m) = g_K \left(\frac{1}{2}\sqrt{1 - 4m^2_{K^\pm}/m^2} + \frac{1}{2}\sqrt{1 - 4m^2_{K^0}/m^2}\right). \quad (12)$$

The fractional coefficients arise from isospin conservation and g_π and g_K are coupling constants for which we take the values:

$$\begin{aligned} g_\pi &= (0.165 \pm 0.010 \pm 0.015)\ \mathrm{GeV}/c^2, \\ g_K &= (4.21 \pm 0.25 \pm 0.21) \times g_\pi, \end{aligned} \quad (13)$$

from results obtained by the BES experiment [55].

The 0^+ component of the $K\pi$ spectrum is not well understood [56,57]; we dub this component $(K\pi)^{*0}_0$ and use the LASS parametrization [56] which consists of the $K^{*0}_0(1430)$ resonance together with an effective range nonresonant component:

$$R_j(m) = \frac{m_{K\pi}}{q\cot\delta_B - iq} + e^{2i\delta_B} \frac{m_0\Gamma_0 \frac{m_0}{q_0}}{(m_0^2 - m^2_{K\pi}) - im_0\Gamma_0 \frac{q}{m_{K\pi}} \frac{m_0}{q_0}}, \quad (14)$$

where $\cot\delta_B = \frac{1}{aq} + \frac{1}{2}rq$. We have used the following values for the scattering length and effective range parameters of this distribution [26]:

$$\begin{aligned} a &= (2.07 \pm 0.10)\ (\mathrm{GeV}/c)^{-1}, \\ r &= (3.32 \pm 0.34)\ (\mathrm{GeV}/c)^{-1}, \end{aligned} \quad (15)$$

and the effective range part of the amplitude is cut off at $m_{K\pi} = 1.8\ \mathrm{GeV}/c^2$. With our final fit model we have determined the preferred values of the a and r parameters and obtain results consistent with those given above. Integrating separately the resonant part, the effective range part, and the coherent sum we find that the $K^{*0}_0(1430)$ resonance accounts for 81%, the effective range term 45%, and destructive interference between the two terms is responsible for the excess 26%.

The nonresonant component of the Dalitz plot is modeled with a constant complex amplitude. We use alternative models [27] to evaluate the model dependence of our results. In these studies we also use the Gounaris-Sakurai form [58] as an alternative model for the $\rho^0(770)$.

For the angular distribution terms T_j we follow the Zemach tensor formalism [59,60]. For the decay of a spin 0 B meson into a spin J resonance and a spin 0 bachelor particle this gives [61]:

$$\begin{aligned} T_j^{J=0} &= 1, \qquad T_j^{J=1} = -2\vec{p}\cdot\vec{q}, \\ T_j^{J=2} &= \tfrac{4}{3}[3(\vec{p}\cdot\vec{q})^2 - (|\vec{p}||\vec{q}|)^2], \end{aligned} \quad (16)$$

where $\vec{p}$ is the momentum of the bachelor particle and $\vec{q}$ is the momentum of the resonance daughter with charge opposite from that of the bachelor particle, both measured in the rest frame of the resonance.

The complex coefficients c_j and $\bar{c}_j$ can be parametrized in various ways that take the possibility of direct *CP* violation into account. We have investigated the choices used in previous studies [27,62] and found that they are susceptible to biases on the fitted parameters, particularly when a resonant contribution is small in magnitude. To ensure the good statistical behavior of our fit, we parametrize the complex coefficients in the following way:

$$\begin{aligned} c_j &= (x_j + \Delta x_j) + i(y_j + \Delta y_j), \\ \bar{c}_j &= (x_j - \Delta x_j) + i(y_j - \Delta y_j). \end{aligned} \quad (17)$$

We have verified that these parameters have approximately Gaussian behavior independent of their true values. In this approach, Δx_j and Δy_j are *CP*-violating parameters.

To allow comparison among experiments we present also fit fractions (FF), defined as the integral of a single decay amplitude squared divided by the coherent matrix element squared for the complete Dalitz plot:

$$FF_j = \frac{\iint(|c_j F_j|^2 + |\bar{c}_j \bar{F}_j|^2) dm^2_{K\pi} dm^2_{\pi\pi}}{\iint(|A|^2 + |\bar{A}|^2) dm^2_{K\pi} dm^2_{\pi\pi}}. \quad (18)$$

The sum of all the fit fractions is not necessarily unity due to the potential presence of net constructive or destructive interference. The CP asymmetry for a given intermediate state is easily determined from the fitted parameters

$$A_{CP,\,j} = \frac{|\bar{c}_j|^2 - |c_j|^2}{|\bar{c}_j|^2 + |c_j|^2} = \frac{-2(x_j \Delta x_j + y_j \Delta y_j)}{x_j^2 + \Delta x_j^2 + y_j^2 + \Delta y_j^2}. \quad (19)$$

The signal Dalitz-plot probability density function (PDF) is formed from the total amplitude as follows:

$$\mathcal{L}_{\rm sig}(m^2_{K\pi}, m^2_{\pi\pi}, q_B) = \frac{\frac{1+q_B}{2}|A|^2\varepsilon + \frac{1-q_B}{2}|\bar{A}|^2\bar{\varepsilon}}{\iint(|A|^2\varepsilon + |\bar{A}|^2\bar{\varepsilon}) dm^2_{K\pi} dm^2_{\pi\pi}}, \quad (20)$$

where q_B is the charge of the B meson candidate and $\varepsilon \equiv \varepsilon(m^2_{K\pi}, m^2_{\pi\pi})$ and $\bar{\varepsilon} \equiv \bar{\varepsilon}(m^2_{K\pi}, m^2_{\pi\pi})$ are the signal reconstruction efficiencies for B^+ and B^- events, respectively, defined for all points in the Dalitz plot.

III. CANDIDATE SELECTION

The B candidates are reconstructed from events that have four or more charged tracks. Each track is required to be well measured and to originate from the beam spot. The B candidates are formed from three-charged-track combinations and particle identification criteria are applied to reject electrons and to separate kaons and pions. In our final state, the average selection efficiency for kaons that have passed the tracking requirements is about 80% including geometrical acceptance, while the average misidentification probability of pions as kaons is about 2%.

Two kinematic variables are used to identify signal B decays. The first variable is

$$\Delta E = E^*_B - \sqrt{s}/2, \quad (21)$$

the difference between the reconstructed CM energy of the B-meson candidate and $\sqrt{s}/2$, where $\sqrt{s}$ is the total CM energy. The second is the energy-substituted mass

$$m_{\rm ES} = \sqrt{(s/2 + \vec{p}_i \cdot \vec{p}_B)^2/E_i^2 - |\vec{p}_B|^2}, \quad (22)$$

where $\vec{p}_B$ is the B momentum and $(E_i,\ \vec{p}_i)$ is the four momentum of the initial state, all measured in the laboratory frame. The $m_{\rm ES}$ distribution for signal events peaks near the B mass with a resolution of around 2.4 MeV/c^2, while the ΔE distribution peaks near zero with a resolution of around 19 MeV. The resolution of ΔE is strongly dependent on the position in the Dalitz plot and so instead of ΔE we use

$$\Delta E' = \frac{\Delta E}{\sigma_{\Delta E}}, \quad (23)$$

where $\sigma_{\Delta E}$ is the error on ΔE, determined separately for each event. This variable exhibits no such dependence. We initially require events to lie in the region formed by the following selection criteria: $5.200 < m_{\rm ES} < 5.286$ GeV/c^2 and $-4.0 < \Delta E' < 15.0$. The region of $\Delta E'$ below -4 is heavily contaminated by four-body B backgrounds and so is not useful for studying the continuum background. The selected region is then subdivided into three areas: the "left sideband" region ($5.20 < m_{\rm ES} < 5.26$ GeV/c^2 and $-4.0 < \Delta E' < 4.0$) used to study the background $\Delta E'$ and Dalitz-plot distributions; the "upper sideband" region ($5.200 < m_{\rm ES} < 5.286$ GeV/c^2 and $7.0 < \Delta E' < 15.0$) used to study the background $m_{\rm ES}$ distributions; and the "signal region" ($5.272 < m_{\rm ES} < 5.286$ GeV/c^2 and $-4.0 < \Delta E' < 4.0$) where the final fit to data is performed. These three regions are illustrated in Fig. 1. Following the calculation of these kinematic variables, each of the B candidates is refitted with its mass constrained to the world average value of the B-meson mass [7] in order to improve the Dalitz-plot position resolution.

The dominant source of background comes from light quark and charm continuum production ($e^+e^- \to q\bar{q}$, where $q = u,\ d,\ s,\ c$). This background is suppressed by requirements on event-shape variables calculated in the CM frame. We compute a neural network (NN) from the following five variables: the ratio of the Legendre polynomial moments L_0 and L_2 [63], the absolute value of the cosine of the angle between the direction of the B and the detector axis, the absolute value of the cosine of the angle between the B thrust axis and the detector axis, the output of a multivariate B-flavor tagging algorithm [64] multiplied by the charge of the B candidate, and the significance

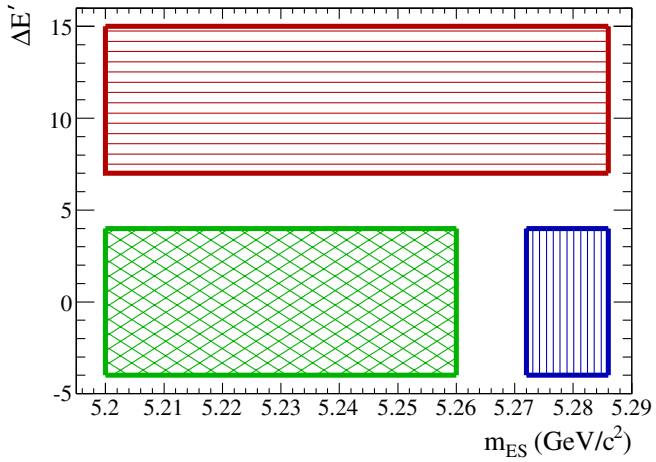

FIG. 1 (color online). Regions of the $\Delta E' - m_{\rm ES}$ plane. The red/horizontal hatching is the "upper sideband," the green/crossed hatching is the "left sideband," and the blue/vertical hatching is the "signal region."

of the measured proper time difference of the B decay vertices. The NN is trained using samples of off-resonance data and signal Monte Carlo (MC) simulated events. The selection requirement placed on the NN output, optimized with MC events, accepts 61% of signal events while rejecting 97% of background events. We see no significant difference between the selection efficiencies of positive and negative candidates.

The reconstruction efficiency distribution over the Dalitz plot is modeled using two-dimensional histograms formed from a sample of around 24×10^6 $B^{\pm} \to K^{\pm}\pi^{\mp}\pi^{\pm}$ MC events. All selection criteria are applied except for those corresponding to the invariant mass veto regions described below. The ratio is taken of two histograms, the denominator containing the true Dalitz-plot distribution of all generated MC events and the numerator containing the reconstructed MC events. The reconstructed events are weighted in order to correct for differences between MC and data in the particle identification and tracking efficiencies. In order to give better resolution near the edges of the Dalitz plot, where most reconstructed events lie, the histograms are formed in the ''square Dalitz plot'' [65] coordinates. Linear interpolation is also applied between bins. The efficiency shows very little variation across the majority of the Dalitz plot but decreases towards the corners where one of the particles has low momentum. The effect of experimental resolution on the signal model is neglected since the resonances under consideration are sufficiently broad. The average reconstruction efficiency for events in the signal box for the nonresonant MC sample is 21.2%. As shown in Eq. (20), in the likelihood fit we use event-by-event efficiencies that depend on the Dalitz-plot position and are different, but consistent, for B^+ and B^- candidates. The fraction of misreconstructed signal events is very small, $\sim$2%, and so such events are not treated explicitly in the signal model.

IV. BACKGROUNDS

In addition to the continuum ($q\bar{q}$) background there are also backgrounds from $B\bar{B}$ events. There are four main sources: (i) combinatorial background from three unrelated tracks; (ii) three- and four-body B decays involving an intermediate D meson; (iii) charmless two- and four-body decays with an extra or missing particle, and (iv) three-body decays with one or more particles misidentified. We veto candidates from charm and charmonium decays with large branching fractions by rejecting events that have invariant masses (in units of GeV/c^2) in the ranges: $1.756 < m_{K^+\pi^-} < 1.931$, $1.660 < m_{\pi^+\pi^-} < 1.800$, $3.019 < m_{\pi^+\pi^-} < 3.179$, and $3.627 < m_{\pi^+\pi^-} < 3.747$. These ranges reject decays from $\bar{D}^0 \to K^+\pi^-$ (or $\pi^+\pi^-$), $J/\psi \to \ell^+\ell^-$ and $\psi(2S) \to \ell^+\ell^-$, respectively, where ℓ is a lepton that has been misidentified.

We study the remaining charm backgrounds that escape the vetoes and the backgrounds from charmless B decays with a large sample of MC-simulated $B\bar{B}$ decays equivalent to approximately 3 times the integrated luminosity of the data sample. Higher-statistics, exclusive MC samples are used to further study 68 B-meson decay modes and to determine the $m_{\rm ES}$, ΔE$'$, and Dalitz-plot distributions that are used in the likelihood fit. These distributions are normalized to the number of predicted events in the final data sample, which we estimate using the reconstruction efficiencies determined from the MC, the number of $B\bar{B}$ pairs in our data sample, and the branching fractions listed by the Particle Data Group [7] and the Heavy Flavor Averaging Group [8]. We further combine modes that have a similar behavior in each of the discriminating variables $m_{\rm ES}$ and ΔE$'$ into a B-background category. For each category combined Dalitz plot, $m_{\rm ES}$ and $\Delta E'$ PDFs are created, and each is included as a separate component in the fit. The predicted yields of $B\bar{B}$ background events in the signal region are 619 ± 17 (659 ± 18) for the negatively (positively) charged sample.

The background Dalitz-plot distributions are included in the likelihood fit through the use of two-dimensional histograms. For backgrounds from B decays these histograms are formed from the various MC samples. For the continuum background the ''left sideband'' data sample is used. This data sideband also contains events from B decays and so MC samples are again used to subtract these events. Like the reconstruction efficiency histograms, those for the backgrounds are formed in the square Dalitz-plot coordinates and have linear interpolation applied between bins. Separate histograms are constructed for B^+ and B^- events. The $q\bar{q}$ and B-background PDFs are identical in their construction and the $q\bar{q}$ PDF is shown here as an example:

$$\mathcal{L}_{q\bar{q}}(m^2_{K\pi}, m^2_{\pi\pi}) = \frac{1}{2}(1 - q_B \mathcal{A}_{q\bar{q}}) \times \left(\frac{\frac{1+q_B}{2} Q(m^2_{K\pi}, m^2_{\pi\pi})}{\iint Q(m^2_{K\pi}, m^2_{\pi\pi}) dm^2_{K\pi} dm^2_{\pi\pi}} + \frac{\frac{1-q_B}{2} \bar{Q}(m^2_{K\pi}, m^2_{\pi\pi})}{\iint \bar{Q}(m^2_{K\pi}, m^2_{\pi\pi}) dm^2_{K\pi} dm^2_{\pi\pi}} \right), \quad (24)$$

where $\mathcal{A}_{q\bar{q}}$ parametrizes possible charge asymmetry in the background, and $Q(m^2_{K\pi}, m^2_{\pi\pi})$ and $\bar{Q}(m^2_{K\pi}, m^2_{\pi\pi})$ are the Dalitz-plot distributions of the $q\bar{q}$ events for B^+ and B^- events, respectively.

V. MAXIMUM LIKELIHOOD FIT

To provide further discrimination between the signal and background hypotheses in the likelihood fit we include PDFs for the kinematic variables $m_{\rm ES}$ and ΔE$'$, which multiply that of the Dalitz plot. The signal is modeled with a double Gaussian function in both cases. The parameters of these functions are obtained from a sample of $K^{\pm}\pi^{\mp}\pi^{\pm}$ MC events and are fixed in the fit to data. The $q\bar{q}$ $m_{\rm ES}$ distribution is modeled with the experimentally moti-

vated ARGUS function [66]. The end point for this ARGUS function is fixed to $\sqrt{s}/2$ and the parameter describing the shape is fixed to the value determined from the "upper sideband." For $\Delta E'$ the continuum is modeled with a linear function, the slope of which is allowed to float in the fit to data. The $B\bar{B}$ background distributions are modeled using histograms obtained from the mixture of $B\bar{B}$ MC samples and are fixed in the fit. The yields of signal and $q\bar{q}$ events are allowed to float in the final fit to the data while the yield of $B\bar{B}$ background events is fixed.

The complete likelihood function is given by:

$$\mathcal{L} = \exp\left(-\sum_k N_k\right) \times \prod_i^{N_e}\left[\sum_k N_k \mathcal{P}_k^i(m_{K\pi}^2, m_{\pi\pi}^2, m_{\rm ES}, \Delta E', q_B)\right], \quad (25)$$

where N_k is the event yield for species k, N_e is the total number of events in the data sample, and $\mathcal{P}_k^i$ is the PDF for species k for event i, which consists of a product of the Dalitz-plot, $m_{\rm ES}$, and $\Delta E'$ PDFs. The function $-\ln\mathcal{L}$ is used in the unbinned fit to the data.

We determine a nominal signal Dalitz-plot model using information from previous studies [26,27,37,67,68] and the change in the fit likelihood value observed when omitting or adding resonances. In our previous study of $B^\pm \to K^\pm\pi^\mp\pi^\pm$ [26] we used a nominal model containing a phase-space nonresonant component and five intermediate resonant states: $K^{*0}(892)\pi^+$, $(K\pi)_0^{*0}\pi^+$, $\rho^0(770)K^+$, $f_0(980)K^+$, and $\chi_{c0}K^+$. With the higher statistics and improved techniques of this analysis, we find it necessary to include additional contributions from $K_2^{*0}(1430)\pi^+$, $f_2(1270)K^+$, and $f_{\rm X}(1300)K^+$ in order to achieve a reasonable agreement of the fit with the data.

The first of these additions improves the agreement in the $K^\pm\pi^\mp$ invariant mass projection; although some discrepancy remains, this cannot be reduced by including other known resonances nor by using alternative forms for the $(K\pi)_0^{*0}$ shape. In the $\pi^\pm\pi^\mp$ invariant mass projection, we find the best agreement to data is achieved by including both the $f_2(1270)K^+$ and $f_{\rm X}(1300)K^+$ terms with X = 0 (i.e. $f_{\rm X}(1300)$ being a scalar). A reasonable fit can be achieved including instead a single broad vector resonance. However, in the case X = 1 it is natural to identify the $f_{\rm X}(1300)$ as the $\rho^0(1450)$, and the observed large ratio of product branching fractions between $\mathcal{B}(B^+ \to \rho^0(1450)K^+) \times \mathcal{B}(\rho^0(1450) \to \pi^+\pi^-)$ and $\mathcal{B}(B^+ \to \rho^0(770)K^+) \times \mathcal{B}(\rho^0(770) \to \pi^+\pi^-)$ leads us to conclude that this cannot be the correct physical interpretation of the data. Note that the $f_2(1270)K^+$ contribution was observed by Belle [27].

In addition, we include a small contribution from $\omega(782)K^+$, which is known to be present based on the well-measured branching fractions of $B^+ \to \omega(782)K^+$ [69,70] and $\omega(782) \to \pi^+\pi^-$ [71]. Although the magnitude of this contribution is known to be very small, due to the narrow width of the $\omega(782)$, it can have a noticeable effect on the $\rho^0(770)$ line shape. Thus, our nominal signal Dalitz-plot model comprises a phase-space nonresonant component and nine intermediate resonance states: $K^{*0}(892)\pi^+$, $(K\pi)_0^{*0}\pi^+$, $K_2^{*0}(1430)\pi^+$, $\rho^0(770)K^+$, $\omega(782)K^+$, $f_0(980)K^+$, $f_2(1270)K^+$, $f_{\rm X}(1300)K^+$, and $\chi_{c0}K^+$. This model differs from that used by Belle [27] by the inclusion of $K_2^{*0}(1430)\pi^+$ and the different parametrization of the $(K\pi)_0^{*0}\pi^+$ and nonresonant terms.

Our choice of parametrization of the $(K\pi)_0^{*0}\pi^+$ and nonresonant terms is motivated by a number of physical considerations. Different parametrizations result in changes in likelihood that are highly dependent on the composition of the rest of the decay model. Compared to our final model, including all resonant terms, the parametrization used by Belle gives a larger fit likelihood. However, this model exhibits large interference between the $K_0^{*0}(1430)$ and nonresonant terms that can be either constructive or destructive, leading to alternative solutions with similar likelihoods but very different values of the fit fractions for these terms. In the case that these terms interfere destructively, the sum of fit fractions far exceeds 100%, which we consider unlikely to be the correct physical description. Moreover, the preferred solution can change depending on the exact composition of the rest of the model—in particular, we find that this problem, which was previously reported by Belle [37], is exacerbated by the presence of the $K_2^{*0}(1430)$. We have also tried a recent proposal for the nonresonant distribution [72] that results in a worse likelihood. Therefore, we use in our nominal model the LASS parametrization for the $(K\pi)_0^{*0}\pi^+$ and a nonresonant term as described above.

The mass and width of the $f_{\rm X}(1300)$ are determined to be $m_{f_{\rm X}} = (1479 \pm 8)$ MeV/c^2, $\Gamma_{f_{\rm X}} = (80 \pm 19)$ MeV, with a correlation of $(-45 \pm 3)\%$, where the errors are statistical only and are determined from a fit to the 2D likelihood profile. These parameters are consistent with the values obtained by Belle [27]: $m_{f_{\rm X}} = (1449 \pm 13)$ MeV/c^2, $\Gamma_{f_{\rm X}} = (126 \pm 25)$ MeV (statistical errors only), and with those listed for the $f_0(1500)$ [7].

We fit 12 753 signal candidates selected from the data using our nominal Dalitz-plot model to obtain the central values of the x_j, Δx_j, y_j, Δy_j parameters for each component. The x and y parameters of the $K^{*0}(892)$ are fixed (to one and zero, respectively) as the reference. The Δx and Δy parameters of the $\omega(782)$ and nonresonant components are fixed to zero in order to improve the fit stability. They are allowed to vary as a cross-check and are found to be consistent with zero. The signal yield, $q\bar{q}$ background yield and asymmetry, and the slope of the $q\bar{q}$ $\Delta E'$ PDF are also floated parameters in the fit. We then generate a large number of MC experiments using the fitted values, and from the spread of results of fits to those experiments determine the statistical uncertainties on those parameters,

TABLE I. Results of fits to data, with statistical, systematic, and model-dependent uncertainties.

Resonance	x	y	Δx	Δy
$K^{*0}(892)\pi^+$	1.0 fixed	0.0 fixed	$-0.017 \pm 0.029 \pm 0.005^{+0.004}_{-0.006}$	$-0.238 \pm 0.228 \pm 0.062^{+0.144}_{-0.018}$
$(K\pi)^{*0}_0\pi^+$	$1.718 \pm 0.084 \pm 0.064^{+0.350}_{-0.055}$	$-0.727 \pm 0.108 \pm 0.080^{+0.331}_{-0.111}$	$-0.154 \pm 0.131 \pm 0.030^{+0.095}_{-0.010}$	$-0.285 \pm 0.337 \pm 0.091^{+0.221}_{-0.019}$
$\rho^0(770)K^+$	$0.683 \pm 0.075 \pm 0.045^{+0.015}_{-0.073}$	$-0.025 \pm 0.135 \pm 0.071^{+0.015}_{-0.073}$	$-0.160 \pm 0.049 \pm 0.024^{+0.094}_{-0.013}$	$0.169 \pm 0.096 \pm 0.057^{+0.133}_{-0.027}$
$f_0(980)K^+$	$-0.220 \pm 0.200 \pm 0.203^{+0.500}_{-0.095}$	$1.203 \pm 0.085 \pm 0.052^{+0.113}_{-0.045}$	$-0.109 \pm 0.143 \pm 0.087^{+0.037}_{-0.103}$	$0.047 \pm 0.045 \pm 0.012^{+0.046}_{-0.018}$
$\chi_{c0}K^+$	$-0.263 \pm 0.044 \pm 0.016^{+0.030}_{-0.014}$	$0.180 \pm 0.052 \pm 0.034^{+0.225}_{-0.022}$	$-0.033 \pm 0.049 \pm 0.012^{+0.017}_{-0.012}$	$-0.007 \pm 0.057 \pm 0.019^{+0.006}_{-0.111}$
Nonresonant	$-0.594 \pm 0.070 \pm 0.170^{+0.112}_{-0.035}$	$0.068 \pm 0.132 \pm 0.154^{+0.112}_{-0.099}$	0.0 fixed	0.0 fixed
$K^{*0}_2(1430)\pi^+$	$-0.301 \pm 0.060 \pm 0.030^{+0.012}_{-0.134}$	$0.424 \pm 0.060 \pm 0.045^{+0.012}_{-0.134}$	$0.032 \pm 0.078 \pm 0.024^{+0.057}_{-0.050}$	$0.007 \pm 0.086 \pm 0.017^{+0.025}_{-0.034}$
$\omega(782)K^+$	$-0.058 \pm 0.067 \pm 0.018^{+0.053}_{-0.011}$	$0.100 \pm 0.051 \pm 0.010^{+0.033}_{-0.032}$	0.0 fixed	0.0 fixed
$f_2(1270)K^+$	$-0.193 \pm 0.043 \pm 0.022^{+0.026}_{-0.033}$	$0.110 \pm 0.050 \pm 0.034^{+0.078}_{-0.073}$	$-0.089 \pm 0.046 \pm 0.019^{+0.034}_{-0.014}$	$0.125 \pm 0.058 \pm 0.021^{+0.034}_{-0.025}$
$f_X(1300)K^+$	$-0.290 \pm 0.047 \pm 0.064^{+0.047}_{-0.031}$	$-0.136 \pm 0.085 \pm 0.098^{+0.102}_{-0.031}$	$0.024 \pm 0.040 \pm 0.019^{+0.023}_{-0.018}$	$0.056 \pm 0.087 \pm 0.044^{+0.010}_{-0.036}$

TABLE II. Summary of measurements of branching fractions (averaged over charge conjugate states) and CP asymmetries. Note that these results are not corrected for secondary branching fractions. The first uncertainty is statistical, the second is systematic, and the third represents the model dependence. The final column is the statistical significance of direct CP violation determined as described in the text.

Mode	Fit fraction (%)	$\mathcal{B}(B^+ \to \text{Mode})(10^{-6})$	A_{CP} (%)	DCPV sig.
$K^+\pi^-\pi^+$ total		$54.4 \pm 1.1 \pm 4.5 \pm 0.7$	$2.8 \pm 2.0 \pm 2.0 \pm 1.2$	
$K^{*0}(892)\pi^+; K^{*0}(892) \to K^+\pi^-$	$13.3 \pm 0.7 \pm 0.7^{+0.4}_{-0.9}$	$7.2 \pm 0.4 \pm 0.7^{+0.3}_{-0.5}$	$+3.2 \pm 5.2 \pm 1.1^{+1.2}_{-0.7}$	0.9σ
$(K\pi)^{*0}_0\pi^+; (K\pi)^{*0}_0 \to K^+\pi^-$	$45.0 \pm 1.4 \pm 1.2^{+12.9}_{-0.2}$	$24.5 \pm 0.9 \pm 2.1^{+7.0}_{-1.1}$	$+3.2 \pm 3.5 \pm 2.0^{+2.7}_{-1.9}$	1.2σ
$\rho^0(770); \rho^0(770)$	$6.54 \pm 0.81 \pm 0.58^{+0.69}_{-0.26}$	$3.56 \pm 0.45 \pm 0.43^{+0.38}_{-0.15}$	$+44 \pm 10 \pm 4^{+5}_{-13}$	3.7σ
$f_0(980)K^+; f_0(980) \to \pi^+\pi^-$	$18.9 \pm 0.9 \pm 1.7^{+2.8}_{-0.6}$	$10.3 \pm 0.5 \pm 1.3^{+1.5}_{-0.4}$	$-10.6 \pm 5.0 \pm 1.1^{+3.4}_{-1.0}$	1.8σ
$\chi_{c0}K^+; \chi_{c0} \to \pi^+\pi^-$	$1.29 \pm 0.19 \pm 0.15^{+0.12}_{-0.03}$	$0.70 \pm 0.10 \pm 0.10^{+0.06}_{-0.02}$	$-14 \pm 15 \pm 3^{+1}_{-5}$	0.5σ
$K^+\pi^-\pi^+$ nonresonant	$4.5 \pm 0.9 \pm 2.4^{+0.6}_{-1.5}$	$2.4 \pm 0.5 \pm 1.3^{+0.3}_{-0.8}$	...	...
$K^{*0}_2(1430)\pi^+; K^{*0}_2(1430) \to K^+\pi^-$	$3.40 \pm 0.75 \pm 0.42^{+0.99}_{-0.13}$	$1.85 \pm 0.41 \pm 0.28^{+0.54}_{-0.08}$	$+5 \pm 23 \pm 4^{+18}_{-7}$	0.2σ
$\omega(782)K^+; \omega(782) \to \pi^+\pi^-$	$0.17 \pm 0.24 \pm 0.03^{+0.05}_{-0.08}$	$0.09 \pm 0.13 \pm 0.02^{+0.03}_{-0.04}$	...	...
$f_2(1270)K^+; f_2(1270) \to \pi^+\pi^-$	$0.91 \pm 0.27 \pm 0.11^{+0.24}_{-0.17}$	$0.50 \pm 0.15 \pm 0.07^{+0.13}_{-0.09}$	$-85 \pm 22 \pm 13^{+22}_{-2}$	3.5σ
$f_X(1300)K^+; f_X(1300) \to \pi^+\pi^-$	$1.33 \pm 0.38 \pm 0.86^{+0.04}_{-0.14}$	$0.73 \pm 0.21 \pm 0.47^{+0.02}_{-0.08}$	$+28 \pm 26 \pm 13^{+7}_{-5}$	0.6σ

as well as the central values and statistical uncertainties on the extracted parameters FF_j and $A_{CP,j}$. This procedure takes into account correlations between the x_j, Δx_j, y_j, Δy_j parameters. In order to make comparisons with previous measurements and predictions from factorization models we multiply each fit fraction by the total branching fraction to calculate the product branching fraction of each mode. The results are shown in Tables I and II. In order to determine the statistical significance of the direct CP violation exhibited by a component we evaluate the difference $\Delta \ln \mathcal{L}$ between the negative log-likelihood of the nominal fit and that of a fit where the Δx and Δy parameters for the given component are fixed to zero. This is then used to evaluate a p-value:

$$p = \int_{2\Delta \ln \mathcal{L}}^{\infty} f(z; n_d) dz, \tag{26}$$

where $f(z; n_d)$ is the χ^2 PDF and n_d is the number of degrees of freedom, two in this case. We then determine the equivalent one-dimensional significance from this p-value. Note that this differs from the significance of $A_{CP,j} \neq 0$, since direct CP violation can be observed in a Dalitz-plot analysis not only through B and $\bar{B}$ amplitudes being different in magnitude, but also by differences in their phases. The significance estimations were cross-checked using MC simulations based on the fit results.

The $K^{\pm}\pi^{\mp}\pi^{\pm}$ signal yield is found to be $4585 \pm 90 \pm 297 \pm 63$ and the total charge asymmetry to be $(2.8 \pm 2.0 \pm 2.0 \pm 1.2)\%$, where the uncertainties are statistical,

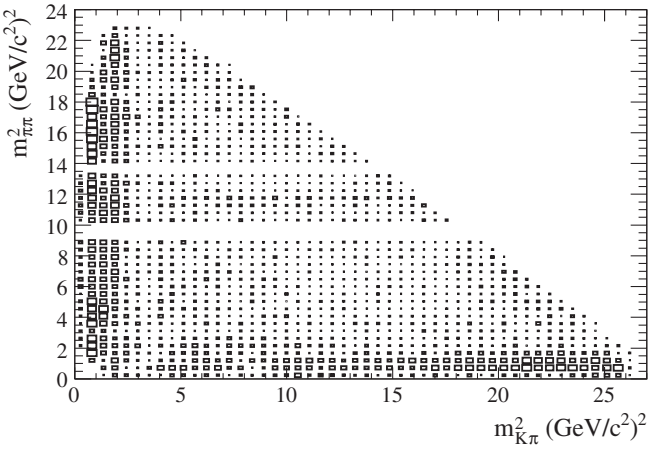

FIG. 2. Background-subtracted Dalitz plot of the combined $B^{\pm} \to K^{\pm}\pi^{\mp}\pi^{\pm}$ data sample in the signal region. The plot shows bins with greater than zero entries. The area of the boxes is proportional to the number of entries. The depleted horizontal bands are the charmonium vetoes.

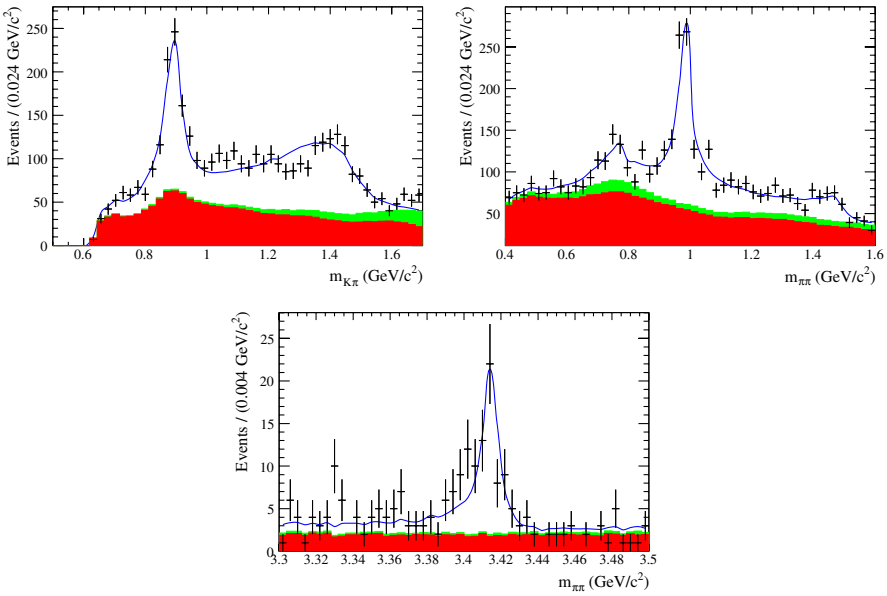

FIG. 3 (color online). Invariant mass projections for the data in the signal region and the fit results. The left-hand plot shows the $m_{K^\pm\pi^\mp}$ spectrum up to 1.7 GeV/c^2. The right-hand plot shows the $m_{\pi^\pm\pi^\mp}$ spectrum up to 1.6 GeV/c^2. The bottom plot shows the $m_{\pi^\pm\pi^\mp}$ spectrum in the region of the χ_{c0}. The data are the black points with statistical error bars, the lower solid (red/dark) histogram is the $q\bar{q}$ component, the middle solid (green/light) histogram is the $B\bar{B}$ background contribution, while the upper blue curve shows the total fit result. For the $m_{K^\pm\pi^\mp}$ plots the requirement is made that $m_{\pi^\pm\pi^\mp}$ is greater than 2 GeV/c^2 and vice versa.

systematic, and model-dependent, respectively. The continuum background yield and charge asymmetry are found to be 6830 ± 110 and $(-2.8 \pm 1.5)\%$, respectively, where the uncertainty is statistical only. The Dalitz plot of the data in the signal region, after subtraction of the two background distributions (using the ${}_s\mathcal{P}lot$ technique [73]), can be seen in Fig. 2. Projections of the data, with the fit result overlaid, onto $K^\pm\pi^\mp$ and $\pi^\pm\pi^\mp$ invariant mass distributions can be seen in Fig. 3. For the $m_{K^\pm\pi^\mp}$ plots the requirement is made that $m_{\pi^\pm\pi^\mp}$ is greater than 2 GeV/c^2 and vice versa in order to better illustrate the structures present. The agreement between the fit result and the data is generally very good, although the discrepancy discussed above is visible in the $m_{K^\pm\pi^\mp}$ spectrum. Using the fitted signal distribution we calculate the average reconstruction efficiency for our signal sample to be 22.5%.

VI. SYSTEMATIC UNCERTAINTIES

The systematic uncertainties that affect the measurement of the fit fractions, phases, and event yields are as follows. The fixed $B\bar{B}$-background yields and asymmetries of the largest categories are allowed to float and the variation of the other fitted parameters is taken as the uncertainty. The effect of the statistics of the MC and data sideband samples used to obtain the fixed shapes of the efficiency, $q\bar{q}$- and $B\bar{B}$-background Dalitz-plot histograms and the $B\bar{B}$-background histograms for $m_{\rm ES}$ and $\Delta E'$ is accounted for by fluctuating independently the histogram bin contents in accordance with their errors and repeating the nominal fit. The uncertainties on how well the samples model these distributions are also taken into account through various cross-checks, including variation of the charm veto range and comparison of continuum shapes between sideband and signal region in MC samples.

The fixed parameters of the signal $m_{\rm ES}$ and $\Delta E'$ PDFs are studied in the control sample $B^+ \to \bar{D}^0\pi^+$; $\bar{D}^0 \to K^+\pi-$. The parameters are determined from MC and data samples, from which biases and scale factors are calculated and used to adjust the parameters for the nominal fit. The parameters are then varied in accordance with the error on these biases and scale factors and the fit repeated. The uncertainties due to fixing the ARGUS parameter of the $q\bar{q}$-background $m_{\rm ES}$ PDF are determined by comparing the results of the fit when the parameter value is obtained from off-peak data.

To confirm the fitting procedure, 500 MC experiments were performed in which the events are generated from the PDFs used in the fit to data. Small fit biases are observed for some of the fit parameters and are included in the systematic uncertainties. The contributions due to particle identification, tracking efficiency corrections, and the calculation of $N_{B\bar{B}}$ are 4.2%, 2.4%, and 1.1%, respectively. The efficiency correction due to the selection requirement on the NN has also been calculated from $B^+ \to \bar{D}^0\pi^+$, $\bar{D}^0 \to K^+\pi-$ data and MC samples, and is found to be 0.979 ± 0.015. The error on this correction is incorporated into the branching fraction systematic uncertainties. Measured CP asymmetries could be affected by detector charge bias. In previous studies [74,75] this effect has been estimated to be very small compared with the precision of our measurements; we take it to be 0.5%.

In addition to the above systematic uncertainties we also estimate effects due to model-dependence, i.e. that characterize the uncertainty on the results due to elements of the signal Dalitz-plot model. The first of these elements consists of the parameters of the various components of the signal model—the masses and widths of all resonances, the effective range and scattering length of the LASS model of the $(K\pi)_0^{*0}$, the coupling constants of the $f_0(980)$ Flatté parametrization, and the value of the Blatt-Weisskopf barrier radius. The associated uncertainties are evaluated by adjusting the parameters within their experimental errors and refitting. The second element is due to the different possible models both for the nonresonant component, which is evaluated by refitting with the parametrization used by Belle [27], and for the $\rho^0(770)$, which is determined by refitting with the Gounaris-Sakurai form. The third element is the uncertainty due to the composition of the signal model. It reflects observed changes in the parameters of the components when the data are fitted with one of the smaller components removed from the model and when the state $K^{*0}(1680)$ is added to the model. The uncertainties from each of these elements are added in quadrature to obtain the final model-dependence.

VII. SUMMARY AND DISCUSSION

Our results are shown in Tables I and II. The total branching fraction $\mathcal{B}(B^+ \to K^+\pi^-\pi^+) = (54.4 \pm 1.1 \pm 4.5 \pm 0.7) \times 10^{-6}$ is compatible with Belle's measurement of $(48.8 \pm 1.1 \pm 3.6) \times 10^{-6}$ [27]. This result was cross-checked by using the same procedure to measure the $B^+ \to \bar{D}^0\pi^+$; $\bar{D}^0 \to K^+\pi^-$ branching fraction, which was found to be consistent with the PDG value [7]. The total charge asymmetry for $B^+ \to K^+\pi^-\pi^+$ has been measured to be consistent with zero to a higher degree of precision than previous measurements.

We see evidence of large direct CP violation in $B^+ \to \rho^0(770)K^+$, consistent with the findings of our previous analysis [26] and of Belle [27]. The statistical significance of the direct CP violation effect is found to be 3.7σ from the change in likelihood when the Δx and Δy terms associated with $\rho^0(770)K^+$ are fixed to zero. We have verified this estimate of the significance using MC simulations. As experimental systematic uncertainties are much smaller than the statistical errors, they do not affect this conclusion. We have cross-checked the effect of the choice of the Dalitz model on the significance. We find that the significance remains above 3σ with alternative models, including that used by Belle [27].

Plots of the $\pi^+\pi^-$ invariant mass projections in the region of the $\rho^0(770)$ and $f_0(980)$ are shown separately for B^+ and B^- candidates in Fig. 4. In an attempt to highlight the direct CP violation effect, we also show plots with the data further subdivided into positive and negative values of $\cos\theta_H = \vec{p}\cdot\vec{q}/(|\vec{p}||\vec{q}|)$, using the notation of Eq. (16). The asymmetry in the excess of events above

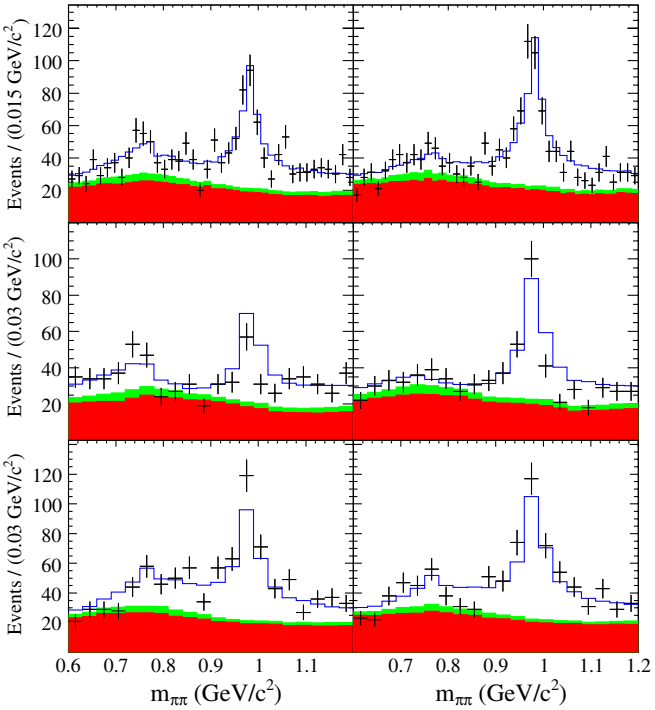

FIG. 4 (color online). Projection plots of the $\pi^+\pi^-$ invariant mass in the region of the $\rho^0(770)$ and $f_0(980)$ resonances. The left (right) plots are for B^- (B^+) candidates. The top row shows all candidates, the middle row shows those where $\cos\theta_H > 0$, and the bottom row shows those where $\cos\theta_H < 0$. The data are the black points with statistical error bars, the lower solid (red/dark) histogram is the $q\bar{q}$ component, the middle solid (green/light) histogram is the $B\bar{B}$ background contribution, while the blue open histogram shows the total fit result.

background in the $\rho^0(770)$ region is particularly apparent in the distributions with the requirement $\cos\theta_H > 0$.

The statistical significance of direct CP violation in $B^+ \to f_2(1270)K^+$ is also above 3σ, but this result suffers from large model uncertainties. The $K^{*0}(892)\pi^+$, $(K\pi)_0^{*0}\pi^+$, and $K_2^{*0}(1430)\pi^+$ charge asymmetries are all consistent with zero, as expected.

After correcting for the secondary branching fraction $\mathcal{B}(K^{*0}(892) \to K^+\pi^-) = \frac{2}{3}$ we find $\mathcal{B}(B^+ \to K^{*0}(892)\pi^+)$ to be $(10.8 \pm 0.6 \pm 1.1^{+0.4}_{-0.8}) \times 10^{-6}$. Similarly we find $\mathcal{B}(B^+ \to f_2(1270)K^+)$ to be $(0.88 \pm 0.26 \pm 0.13^{+0.23+0.01}_{-0.16-0.02}) \times 10^{-6}$ and $\mathcal{B}(B^+ \to K_2^{*0}(1430)\pi^+)$ to be $(5.6 \pm 1.2 \pm 0.8^{+1.6}_{-0.2} \pm 0.1) \times 10^{-6}$, where the fourth errors are due to the uncertainties on the secondary branching fractions. These and the other branching fraction measurements are, in general, consistent with previous measurements. The product branching fraction of $B^+ \to \omega(782)K^+$; $\omega(782) \to \pi^+\pi^-$ agrees with the expectation from previous measurements, albeit with large uncertainties. The only disparities between our results and those reported by Belle [27] arise from the different treatments of the $K^+\pi^-$ S-wave. The forward-backward asymmetry apparent in both the $K^{*0}(892)$ and $f_0(980)$ bands in

Fig. 2 is well reproduced by the fit and is due to S–P-wave interference in the Dalitz plot.

The $(K\pi)_0^{*0}$ component is modeled in our analysis by the LASS parametrization [56], which consists of a nonresonant effective range term plus a relativistic Breit-Wigner term for the $K_0^{*0}(1430)$ resonance itself. This parametrization makes use of the available experimental information, however the size of the phase space here means that the range of $K^+\pi^-$ invariant masses under consideration is much greater than in previous studies. The agreement between the model and the data in the region of the $K_0^{*0}(1430)$ is not as good as in the remainder of the Dalitz plot but all alternative models tried yielded poorer results. If we assume that the model used is correct then we can calculate the branching fraction for $B^+ \to K_0^{*0}(1430)\pi^+$ and find it to be: $(32.0 \pm 1.2 \pm 2.7^{+9.1}_{-1.4} \pm 5.2) \times 10^{-6}$, where the fourth error is due to the uncertainty on the branching fraction of $K_0^{*0}(1430) \to K\pi$ combined with the uncertainty on the proportion of the $(K\pi)_0^{*0}$ component due to the $K_0^{*0}(1430)$ resonance. In addition we can calculate the total nonresonant contribution by combining coherently the nonresonant part of the LASS parametrization and the phase-space nonresonant. We find this total nonresonant branching fraction to be: $(9.3 \pm 1.0 \pm 1.2^{+6.7}_{-0.4} \pm 1.2) \times 10^{-6}$, where the fourth error is due to the uncertainty on the proportion of the $(K\pi)_0^{*0}$ component that is nonresonant. The Belle collaboration finds somewhat larger $K_0^{*0}(1430)$ and nonresonant branching fractions though they treat the $K_0^{*0}(1430)$ as a Breit-Wigner component, separate from the rest of the S-wave modeled as a nonresonant amplitude that has variation in magnitude but no variation in phase over the Dalitz plot [27].

In conclusion, we have performed a Dalitz-plot analysis of $B^\pm \to K^\pm\pi^\mp\pi^\pm$ decays based on a 347.5 fb^{-1} data sample containing $(383.2 \pm 4.2) \times 10^6$ $B\bar{B}$ pairs collected by the *BABAR* detector. To obtain a good fit to the data we find that contributions from $f_2(1270)K^+$ and $f_X(1300)K^+$ are necessary, with $f_X(1300)$ being a scalar with parameters $m_{f_X} = (1479 \pm 8)$ MeV/c^2, $\Gamma_{f_X} = (80 \pm 19)$ MeV, with a correlation of $(-45 \pm 3)\%$, where the errors are statistical only. These are consistent with the mass and width of the $f_0(1500)$. In the $K^\pm\pi^\mp$ invariant mass projection some discrepancy remains in the 1200–1400 MeV/c^2 range—our model includes $(K\pi)_0^{*0}\pi^+$ (using the LASS parametrization) and $K_2^{*0}(1430)\pi^+$ terms in this region, although some alternative models also give a good description of the data. We measure *CP*-averaged branching fractions and direct *CP* asymmetries for intermediate resonant and nonresonant contributions. Our results are consistent with the standard model, and can be used together with results from other $B \to K\pi\pi$ decays to obtain constraints on the Cabibbo-Kobayashi-Maskawa (CKM) phase γ. We find evidence for direct *CP* violation in the decay $B^\pm \to \rho^0(770)K^\pm$, with a *CP*-violation parameter $A_{CP} = (+44 \pm 10 \pm 4^{+5}_{-13})\%$. These results supersede those in our previous publication [26].

ACKNOWLEDGMENTS

We are grateful for the extraordinary contributions of our PEP-II colleagues in achieving the excellent luminosity and machine conditions that have made this work possible. The success of this project also relies critically on the expertise and dedication of the computing organizations that support *BABAR*. The collaborating institutions wish to thank SLAC for its support and the kind hospitality extended to them. This work is supported by the U.S. Department of Energy and National Science Foundation, the Natural Sciences and Engineering Research Council (Canada), the Commissariat à l'Energie Atomique and Institut National de Physique Nucléaire et de Physique des Particules (France), the Bundesministerium für Bildung und Forschung and Deutsche Forschungsgemeinschaft (Germany), the Istituto Nazionale di Fisica Nucleare (Italy), the Foundation for Fundamental Research on Matter (The Netherlands), the Research Council of Norway, the Ministry of Education and Science of the Russian Federation, Ministerio de Educación y Ciencia (Spain), and the Science and Technology Facilities Council (United Kingdom). Individuals have received support from the Marie-Curie IEF program (European Union) and the A. P. Sloan Foundation.

[1] M. Kobayashi and T. Maskawa, Prog. Theor. Phys. **49**, 652 (1973).
[2] A. Alavi-Harati *et al.* (KTeV Collaboration), Phys. Rev. Lett. **83**, 22 (1999).
[3] V. Fanti *et al.* (NA48 Collaboration), Phys. Lett. B **465**, 335 (1999).
[4] B. Aubert *et al.* (*BABAR* Collaboration), Phys. Rev. Lett. **87**, 091801 (2001).
[5] K. Abe *et al.* (Belle Collaboration), Phys. Rev. Lett. **87**, 091802 (2001).
[6] B. Aubert *et al.* (*BABAR* Collaboration), Phys. Rev. Lett. **93**, 131801 (2004).
[7] W. M. Yao *et al.* (Particle Data Group), J. Phys. G **33**, 1 (2006).
[8] E. Barberio *et al.* (Heavy Flavor Averaging Group (HFAG)), arXiv:0704.3575.

[9] B. Aubert *et al.* (*BABAR* Collaboration), Phys. Rev. D **76**, 091102 (2007).
[10] S. W. Lin *et al.* (Belle Collaboration), Nature (London) **452**, 332 (2008).
[11] A. J. Buras, R. Fleischer, S. Recksiegel, and F. Schwab, Phys. Rev. Lett. **92**, 101804 (2004).
[12] A. J. Buras, R. Fleischer, S. Recksiegel, and F. Schwab, Eur. Phys. J. C **45**, 701 (2006).
[13] S. Baek, P. Hamel, D. London, A. Datta, and D. A. Suprun, Phys. Rev. D **71**, 057502 (2005).
[14] C. S. Kim, S. Oh, and C. Yu, Phys. Rev. D **72**, 074005 (2005).
[15] X.-Q. Li and Y.-D. Yang, Phys. Rev. D **72**, 074007 (2005).
[16] H.-N. Li, S. Mishima, and A. I. Sanda, Phys. Rev. D **72**, 114005 (2005).
[17] C.-H. Chen, Phys. Lett. B **525**, 56 (2002).
[18] D.-S. Du, H.-J. Gong, J.-F. Sun, D.-S. Yang, and G.-H. Zhu, Phys. Rev. D **65**, 094025 (2002).
[19] M. Beneke and M. Neubert, Nucl. Phys. B **675**, 333 (2003).
[20] C.-W. Chiang, M. Gronau, Z. Luo, J. L. Rosner, and D. A. Suprun, Phys. Rev. D **69**, 034001 (2004).
[21] C. Isola, M. Ladisa, G. Nardulli, and P. Santorelli, Phys. Rev. D **68**, 114001 (2003).
[22] X.-Q. Li and Y.-D. Yang, Phys. Rev. D **73**, 114027 (2006).
[23] H.-N. Li and S. Mishima, Phys. Rev. D **74**, 094020 (2006).
[24] B. El-Bennich, A. Furman, R. Kaminski, L. Lesniak, and B. Loiseau, Phys. Rev. D **74**, 114009 (2006).
[25] W. Wang, Y.-M. Wang, D.-S. Yang, and C.-D. Lu, arXiv:0801.3123.
[26] B. Aubert *et al.* (*BABAR* Collaboration), Phys. Rev. D **72**, 072003 (2005); **74**, 099903(E) (2006).
[27] A. Garmash *et al.* (Belle Collaboration), Phys. Rev. Lett. **96**, 251803 (2006).
[28] A. Garmash *et al.* (Belle Collaboration), Phys. Rev. D **75**, 012006 (2007).
[29] B. Aubert *et al.* (*BABAR* Collaboration), arXiv:0708.2097.
[30] B. Aubert *et al.* (*BABAR* Collaboration), arXiv:0711.4417.
[31] H. J. Lipkin, Y. Nir, H. R. Quinn, and A. Snyder, Phys. Rev. D **44**, 1454 (1991).
[32] N. G. Deshpande, N. Sinha, and R. Sinha, Phys. Rev. Lett. **90**, 061802 (2003).
[33] M. Ciuchini, M. Pierini, and L. Silvestrini, Phys. Rev. D **74**, 051301 (2006).
[34] M. Gronau, D. Pirjol, A. Soni, and J. Zupan, Phys. Rev. D **75**, 014002 (2007).
[35] M. Gronau, D. Pirjol, A. Soni, and J. Zupan, Phys. Rev. D **77**, 057504 (2008).
[36] I. Bediaga, G. Guerrer, and J. M. de Miranda, Phys. Rev. D **76**, 073011 (2007).
[37] A. Garmash *et al.* (Belle Collaboration), Phys. Rev. D **71**, 092003 (2005).
[38] B. Aubert *et al.* (*BABAR* Collaboration), Phys. Rev. D **74**, 032003 (2006).
[39] B. Aubert *et al.* (*BABAR* Collaboration), Phys. Rev. Lett. **99**, 161802 (2007).
[40] B. Aubert *et al.* (*BABAR* Collaboration), Phys. Rev. Lett. **99**, 221801 (2007).
[41] P. Minkowski and W. Ochs, Eur. Phys. J. C **39**, 71 (2005).
[42] A. Furman, R. Kaminski, L. Lesniak, and B. Loiseau, Phys. Lett. B **622**, 207 (2005).
[43] H.-Y. Cheng, C.-K. Chua, and K.-C. Yang, Phys. Rev. D **73**, 014017 (2006).
[44] Z.-G. Wang, Nucl. Phys. A **791**, 106 (2007).
[45] H.-Y. Cheng, C.-K. Chua, and A. Soni, Phys. Rev. D **76**, 094006 (2007).
[46] E. Klempt and A. Zaitsev, Phys. Rep. **454**, 1 (2007).
[47] B. Aubert *et al.* (*BABAR* Collaboration), Nucl. Instrum. Methods Phys. Res., Sect. A **479**, 1 (2002).
[48] W. Kozanecki, Nucl. Instrum. Methods Phys. Res., Sect. A **446**, 59 (2000).
[49] G. N. Fleming, Phys. Rev. **135**, B551 (1964).
[50] D. Morgan, Phys. Rev. **166**, 1731 (1968).
[51] D. Herndon, P. Soding, and R. J. Cashmore, Phys. Rev. D **11**, 3165 (1975).
[52] J. Blatt and V. E. Weisskopf, *Theoretical Nuclear Physics* (Wiley, New York, 1952).
[53] D. V. Bugg (private communication).
[54] S. M. Flatté, Phys. Lett. B **63**, 224 (1976).
[55] M. Ablikim *et al.* (BES Collaboration), Phys. Lett. B **607**, 243 (2005).
[56] D. Aston *et al.* (LASS Collaboration), Nucl. Phys. **B296**, 493 (1988).
[57] D. V. Bugg, Phys. Lett. B **572**, 1 (2003).
[58] G. J. Gounaris and J. J. Sakurai, Phys. Rev. Lett. **21**, 244 (1968).
[59] C. Zemach, Phys. Rev. **133**, B1201 (1964).
[60] C. Zemach, Phys. Rev. **140**, B97 (1965).
[61] D. Asner, arXiv:hep-ex/0410014.
[62] D. M. Asner *et al.* (CLEO Collaboration), Phys. Rev. D **70**, 091101 (2004).
[63] B. Aubert *et al.* (*BABAR* Collaboration) Phys. Rev. Lett. **89**, 281802 (2002).
[64] B. Aubert *et al.* (*BABAR* Collaboration), Phys. Rev. Lett. **93**, 231801 (2004).
[65] B. Aubert *et al.* (*BABAR* Collaboration), Phys. Rev. D **76**, 012004 (2007).
[66] H. Albrecht *et al.* (ARGUS Collaboration), Z. Phys. C **48**, 543 (1990).
[67] K. Abe *et al.* (Belle Collaboration), Phys. Rev. D **65**, 092005 (2002).
[68] B. Aubert *et al.* (*BABAR* Collaboration), Phys. Rev. D **70**, 092001 (2004).
[69] B. Aubert *et al.* (*BABAR* Collaboration), Phys. Rev. D **76**, 031103 (2007).
[70] C. M. Jen *et al.* (Belle Collaboration), Phys. Rev. D **74**, 111101 (2006).
[71] R. R. Akhmetshin *et al.* (CMD-2 Collaboration), Phys. Lett. B **648**, 28 (2007).
[72] I. Bediaga, D. R. Boito, G. Guerrer, F. S. Navarra, and M. Nielsen, arXiv:0709.0075.
[73] M. Pivk and F. R. Le Diberder, Nucl. Instrum. Methods Phys. Res., Sect. A **555**, 356 (2005).
[74] B. Aubert *et al.* (*BABAR* Collaboration), Phys. Rev. D **71**, 111101 (2005).
[75] B. Aubert *et al.* (*BABAR* Collaboration), Phys. Rev. Lett. **99**, 021603 (2007).